

Electronic Supporting Information (ESI)

for

From energy to electron transfer photocatalysis (*PenT*→*PET*): oxidative cyclobutane cleavage alters the product composition

J. Lefarth,^a A. Haseloer,^b L. Kletsch,^b A. Klein,^b J. Neudörfl,^a A. G. Griesbeck^{a*}

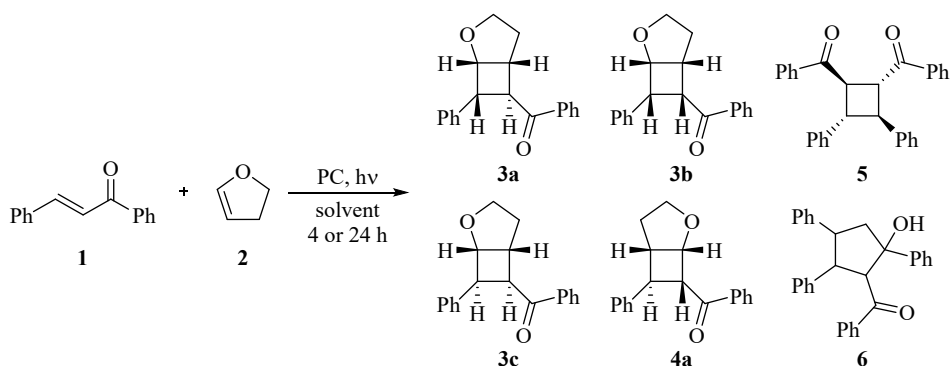
University of Cologne, Faculty of Mathematics and Natural Sciences, Department of Chemistry, Greinstr. 4-6, D-50939 Köln, Germany

*E-Mail: griesbeck@uni-koeln.de; ^a Organic Chemistry; ^b Inorganic Chemistry.

Contents

1. Catalytic screening experiments	S1
2. Cyclic voltammetry	S3
3. Spectroelectrochemistry	S6
4. Crystal structure analysis	S7
5. ¹³ C-NMR structure analysis	S9
5. References	S10

1. Catalytic screening experiments



A 10 mL Pyrex tube with a small stirring bar was charged with the solvent (5.0 mL) and 26 eq. 2,3-dihydrofuran (**2**, 1.0 mL) for an enone concentration of $c = 83.3$ mM. The reaction mixture was degassed with argon for 15-30 min after which chalcone (**1**, 0.5 mmol) and, if used, either 5.6 mg (1 mol%) [Ir-F] or 54 mg (40 mol%) MK was added. The reaction mixture was irradiated for 4 or 24 h with blue LEDs (LED PowerBar V2, Lumitronix, $P_{\text{total}} = 11$ W, $\lambda_{\text{max}} = 455$ nm) or a photoreactor from Rayonet (16 UV-A lamps, $P_{\text{total}} = 128$ W (8 W per lamp), $\lambda_{\text{max}} = 350$ nm). Afterwards, the crude reaction mixture was filtered (SiO_2 , EtOAc) and analysed by GC-MS. The data is summarised in Tables S1-S3.¹

Table S1 Solvent screening using MK^a

entry	solvent	yield [%] ^b				
		total	3a	3b	5	6
2	MeCN	97	26	13	<1	42
3^c	MeCN	9	3	<1	<1	3
10	benzene	96	2	7	3	80
7	toluene	95	1	15	—	71
11	cyclohexane	81	9	6	42	19
12	DCM	98	15	17	—	58
13	1,4-dioxane	98	<1	5	—	88
14	Et ₂ O	62	5	2	18	35
15	acetone	99	7	14	—	73
16	EtOAc	97	7	9	—	75
17	<i>i</i> -PrOH	80	29	8	12	21
18	EtOH	13	9	<1	1	2
19	MeOH	14	10	<1	<1	2
20	MeNO ₂	6	3	<1	—	—
21	water	7	1	<1	3	3
22	MeCN:water ^d	21	5	1	1	13

^a With chalcone (**1**, 83 mM, 0.5 mmol), 2,3-DHF (**2**, 26 eq.), 40 mol% MK, irradiation at $\lambda = 350$ nm for 24 h under argon atmosphere. ^b Determined by GC-MS analysis. ^c Irradiated for 4 h. ^d MeCN:water mixture of 9:1.

Table S2 Solvent screening by direct excitation of chalcone **1**^a

entry	solvent	yield [%] ^b				
		total	3a	3b	5	6
1^c	MeCN	51	23	8	3	-
6	toluene	83	16	14	26	-
23	1,4-dioxane	26	10	3	4	-
24	acetone	17	11	2	1	-

^a Using **1**, (83 mM) and 2,3-DHF (**2**, 26 eq.) in 5 mL MeCN at $\lambda = 350$ nm for 24 h under argon atmosphere. ^b Determined by GC-MS analysis. ^c Mean value of four experiments.

Table S3 Solvent screening using [Ir-F]^a

entry	solvent	t [h]	yield [%] ^b				
			total	3a	3b	5	6
4	MeCN	24	>99	33	44	<1	1
5 ^c	MeCN	4	98	50	14	10	4
8	toluene	24	99	23	37	13	13
9	toluene	4	73	18	5	32	5
25	cyclohexane	4	61	9	3	4	-
26	DCM	4	76	30	8	20	2
27	1,4-dioxane	24	98	4	34	-	55
28	1,4-dioxane	4	94	31	9	23	11
29	acetone	24	99	32	48	<1	6
30	EtOAc	24	99	5	21	-	68
31	EtOAc	4	94	31	9	17	19
32	EtOH	4	97	47	13	7	9
33	HFIP ^d	4	61	3	<1	56	2

^a Chalcone (**1**, 83 mM), 2,3-DHF (**2**, 26 eq.), 1 mol% [Ir-F], irradiation with blue LEDs under argon atmosphere.^b Determined by GC-MS analysis.^c Mean value of four experiments.^d HFIP = hexafluoroisopropanol.

2. Cyclic voltammetry

Cyclic voltammograms (CV) were measured under an argon atmosphere in extra dry MeCN with 0.1 M *n*Bu₄NPF₆ as electrolyte and referenced to the ferrocene/ferrocenium couple as an internal standard (Fc/Fc⁺). The three electrodes consisted of a glassy carbon working electrode, a platinum counter electrode and an Ag/AgCl pseudo reference electrode. The scan rate was 100 mV/s if not stated otherwise. The recording was performed with a Metrohm *Autolab PG STAT* potentiostat.

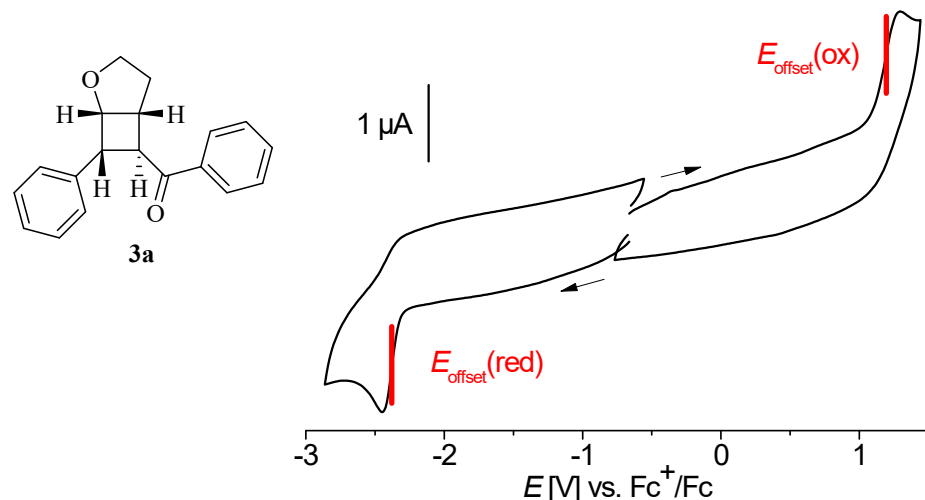


Fig. S1 Cyclic voltammograms of cyclobutane **3a** in 0.1 M *n*Bu₄NPF₆/MeCN. Offset potentials (E_{offset}) marked in red represent the approximated half-wave potentials.

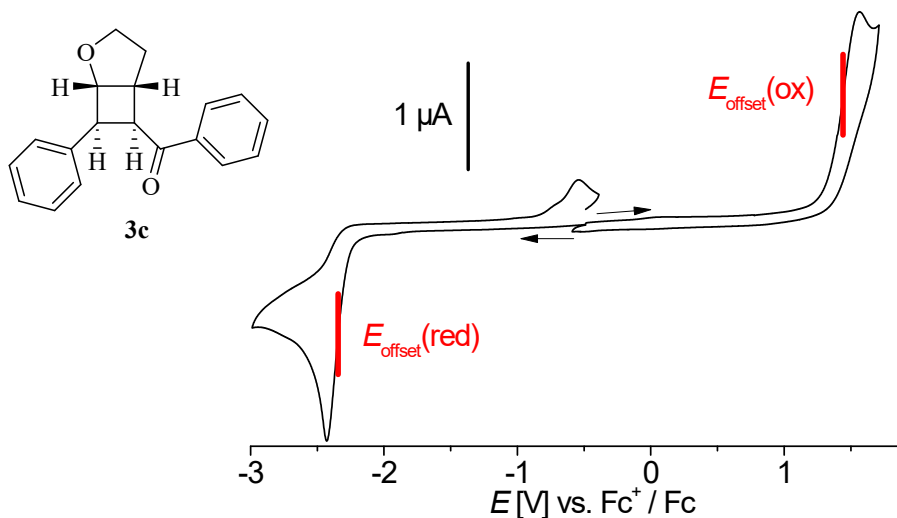


Fig. S2 Cyclic voltammograms of cyclobutane **3c** in 0.1 M $n\text{Bu}_4\text{NPF}_6$ /MeCN. Offset potentials (E_{offset}) marked in red represent the approximated half-wave potentials.

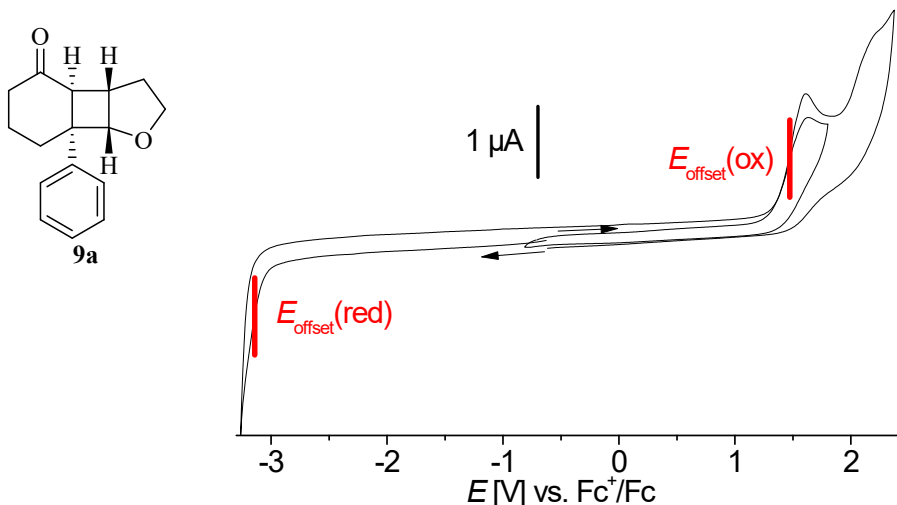


Fig. S3 Cyclic voltammograms of cyclobutane **9a** in 0.1 M $n\text{Bu}_4\text{NPF}_6$ /MeCN. Offset potentials (E_{offset}) marked in red represent the approximated half-wave potentials.

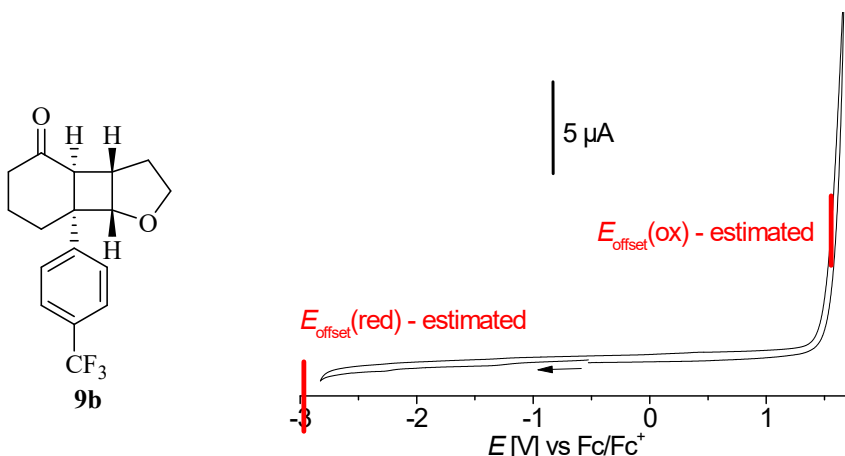


Fig. S4 Cyclic voltammograms of cyclobutane **9b** in 0.1 M $n\text{Bu}_4\text{NPF}_6$ /MeCN. Estimated offset potentials (E_{offset} -estimated) marked in red represent the maximum half-wave potentials.

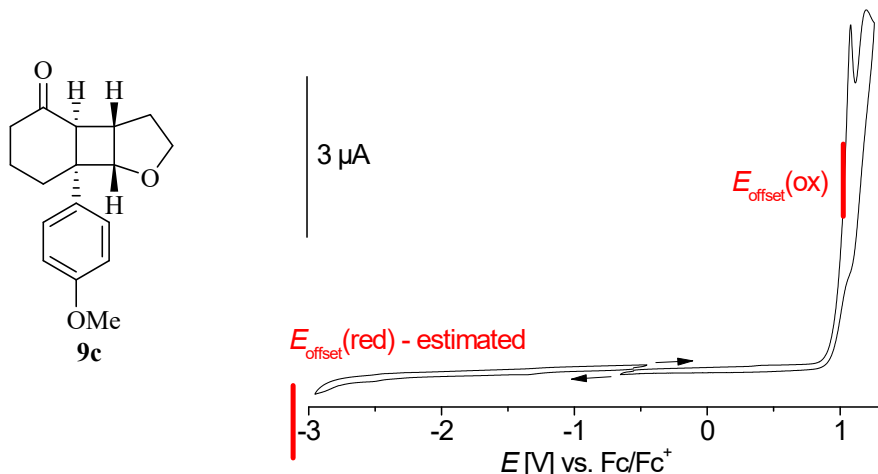


Fig. S5 Cyclic voltammograms of cyclobutane **9c** in 0.1 M $n\text{Bu}_4\text{NPF}_6/\text{MeCN}$. Offset potentials (E_{offset}) marked in red represent the approximated half-wave potentials. Estimated offset potentials ($E_{\text{offset}} - \text{estimated}$) marked in red represent the maximum half-wave potentials.

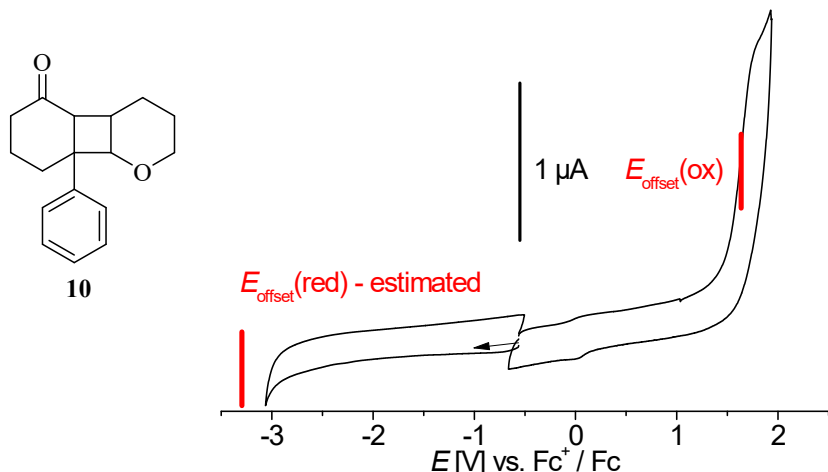


Fig. S6 Cyclic voltammogram of cyclobutane **10** in 0.1 M $n\text{Bu}_4\text{NPF}_6/\text{MeCN}$. Offset potentials (E_{offset}) marked in red represent the approximated half-wave potentials. Estimated offset potentials ($E_{\text{offset}} - \text{estimated}$) marked in red represent the maximum half-wave potentials.

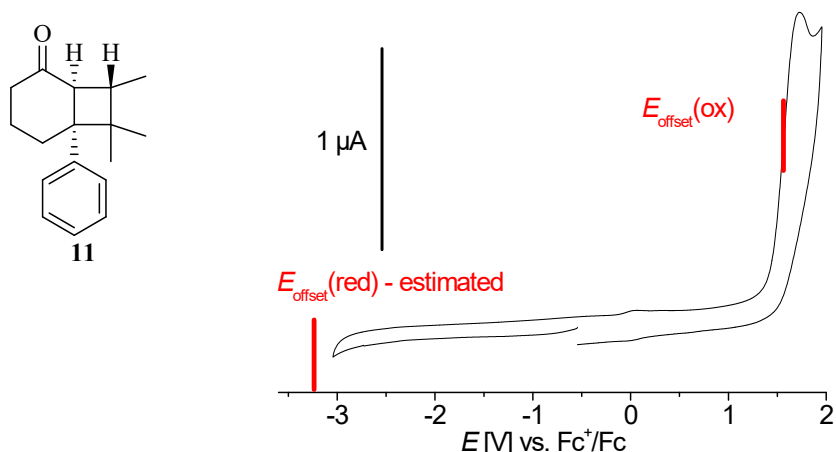


Fig. S7 Cyclic voltammogram of cyclobutane **11** in 0.1 M $n\text{Bu}_4\text{NPF}_6/\text{MeCN}$. Offset potentials (E_{offset}) marked in red represent the approximated half-wave potentials. Estimated offset potentials ($E_{\text{offset}} - \text{estimated}$) marked in red represent the maximum half-wave potentials.

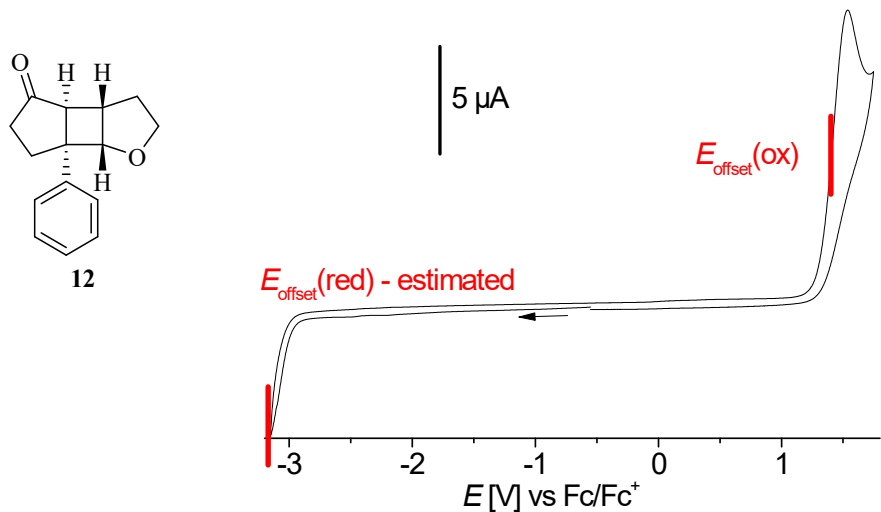


Fig. S8 Cyclic voltammogram of cyclobutane **12** in 0.1 M $n\text{Bu}_4\text{NPF}_6/\text{MeCN}$. Offset potentials (E_{offset}) marked in red represent the approximated half-wave potentials. Estimated offset potentials ($E_{\text{offset}} - \text{estimated}$) marked in red represent the maximum half-wave potentials.

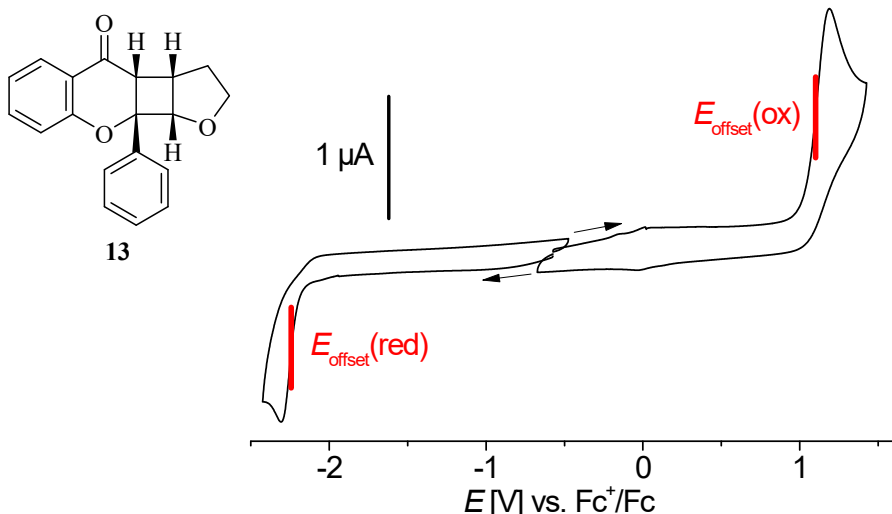


Fig. S9 Cyclic voltammograms of cyclobutane **13** in 0.1 M $n\text{Bu}_4\text{NPF}_6/\text{MeCN}$. Offset potentials (E_{offset}) marked in red represent the approximated half-wave potentials.

3. Spectroelectrochemistry

The spectra were recorded under an argon atmosphere in extra dry MeCN with 0.1 M ($n\text{Bu}_4\text{N}$)(PF_6) as electrolyte in an *OTTLE*-cell (optical thin layer electrochemical cell)² using *Varian 50 Scan UV-visible* spectrophotometer. Typically, the voltage was increased in 100 mV steps over a broad range of potentials and in 10 mV steps close to the potentials of the redox events (from CV). UV-vis absorption spectra measured after 1 min at each potential.^{3,4}

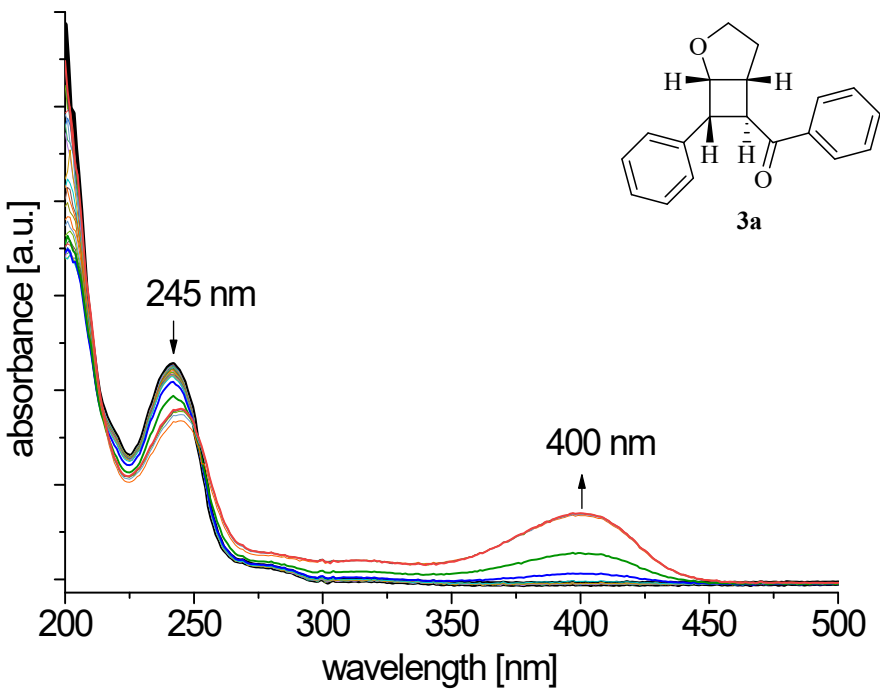


Fig. S10 Spectroelectrochemistry of cyclobutane **3a** in $0.1 \text{ M } n\text{Bu}_4\text{NPF}_6/\text{MeCN}$ upon anodic oxidation in the range 0 to 1.3 V vs. ferrocene/ferrocenium.

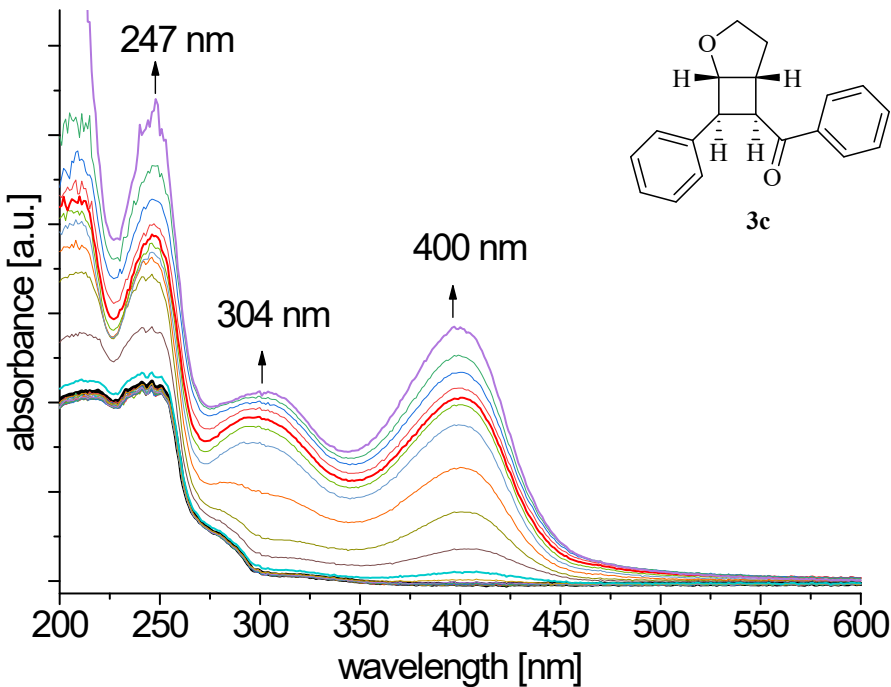


Fig. S11 Spectroelectrochemistry of cyclobutane **3c** $0.1 \text{ M } n\text{Bu}_4\text{NPF}_6/\text{MeCN}$ upon anodic oxidation in the range 0 to 1.5 V.

4. Crystal structure analysis

Single crystal X-ray structure data was determined at 100 K on a Nonius Kappa CCD four-circle diffractometer from *Bruker* with molybdenum source or a D8 Venture with copper microfocus source. The structures were refined using SHELXT and SHELXL.⁵ Selected metrics of the cyclobutane

structures (Fig. S10) are listed in Tables S4 and S5, full structural data and results of the structure solution and refinement can be obtained from the CCSD data base (for entry numbers, see Tables S4-S6).

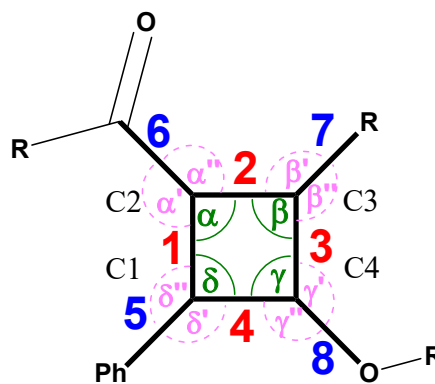


Fig. S10 Nomenclature for the crystal structure analysis summarised in Table S4-S6.

Table S4 Selected bond angles for cyclobutanes from crystal structure analysis.

angles (°)	3c	9a	9b	9c_1	9c_2	9c_3	9c_4	11	13
α	90.60(9)	89.44(1)	88.92(11)	89.4(2)	89.9(2)	90.0(2)	89.7(2)	88.00(7)	91.10(8)
β	89.54(9)	90.14(1)	89.44(12)	90.5(2)	90.2(2)	90.3(2)	90.5(2)	88.22(7)	89.28(8)
γ	91.26(9)	90.19(1)	89.25(11)	90.3(2)	90.2(2)	90.2(2)	90.2(2)	87.11(7)	90.67(8)
δ	88.08(8)	89.65(1)	89.52(11)	89.3(2)	89.2(2)	89.2(2)	89.1(2)	87.82(7)	88.54(8)
α'	117.01(10)	119.46(1)	120.65(12)	120.3(2)	119.5(3)	119.4(2)	120.0(3)	120.23(8)	116.86(9)
α''	117.62(10)	114.43(1)	116.30(13)	112.7(2)	113.9(2)	113.0(2)	112.6(2)	118.01(9)	119.94(9)
β'	115.73(10)	114.76(1)	115.16(13)	113.9(2)	114.3(3)	114.6(2)	114.4(2)	118.54(8)	119.14(9)
β''	103.68(9)	104.15(1)	104.34(13)	104.6(2)	104.1(2)	104.2(2)	104.3(2)	120.69(9)	103.80(9)
γ'	107.55(9)	107.23(1)	107.01(12)	107.0(2)	107.3(2)	107.3(2)	107.3(2)	116.32(9)	108.81(8)
γ''	114.97(9)	117.45(1)	117.20(13)	118.2(2)	118.1(2)	118.2(2)	118.4(2)	118.62(8)	116.32(9)
δ'	116.12(10)	118.54(1)	117.90(12)	114.0(2)	115.4(2)	116.0(2)	115.0(2)	117.42(8)	116.01(8)
δ''	116.84(10)	116.01(1)	116.82(12)	118.4(2)	118.5(2)	117.5(2)	117.4(2)	117.94(8)	118.44(9)
δ'''		109.73(1)	111.38(12)	110.9(2)	110.5(2)	110.1(2)	110.5(2)	112.84(8)	109.51(8)
δ''''		110.66(1)	108.33(12)	111.7(2)	111.7(2)	111.6(2)	111.8(2)	109.60(8)	108.92(8)
δ'''''		110.89(1)	111.01(12)	111.0(2)	110.0(2)	111.1(2)	111.7(2)	109.70(8)	113.85(8)
γ'''								112.19(8)	116.51(8)
γ''''								112.02(8)	108.37(8)
CCDC number	2192929	2192930	2192931	2192933	2192933	2192933	2192933	2192932	2089434 ⁶

Table S5 Selected bond length for cyclobutanes from crystal structure analysis.

bond length (Å)	3c	9a	9b	9c_1	9c_2	9c_3	9c_4	11	13
1	1.5844(17)	1.5663(1)	1.558(2)	1.574(4)	1.568(4)	1.571(4)	1.574(4)	1.5553(14)	1.5550(14)
2	1.5467(16)	1.5666(1)	1.569(2)	1.566(4)	1.567(4)	1.564(4)	1.564(4)	1.5666(14)	1.5628(15)
3	1.5553(17)	1.5494(1)	1.554(2)	1.547(4)	1.551(4)	1.551(4)	1.549(4)	1.5622(15)	1.5506(15)
4	1.5584(16)	1.5630(1)	1.564(2)	1.571(4)	1.577(4)	1.577(4)	1.575(4)	1.5849(14)	1.5787(15)
5	1.5035(17)	1.5140(1)	1.508(2)	1.514(4)	1.509(4)	1.504(4)	1.513(4)	1.5155(14)	1.5147(14)
6	1.5038(16)	1.4991(1)	1.510(2)	1.491(4)	1.493(4)	1.499(4)	1.497(4)	1.5056(14)	1.5070(15)
7	1.5248(17)	1.5217(1)	1.521(2)	1.522(4)	1.517(4)	1.523(4)	1.516(4)	1.5173(14)	1.5310(15)
8	1.4239(15)	1.4207(1)	1.417(2)	1.418(4)	1.417(4)	1.421(4)	1.417(4)	1.5283(15)	1.4077(13)
5'		1.5483(1)	1.546(2)	1.539(4)	1.549(4)	1.538(4)	1.537(4)	1.5405(14)	1.4372(13)
8'								1.5247(15)	
CCDC number	2192929	2192930	2192931	2192933	2192933	2192933	2192933	2192932	2089434 ⁶

Table S6 Selected dihedral angles for cyclobutanes from crystal structure analysis.

dihedral angle (°)	3c	9a	9b	9c_1	9c_2	9c_3	9c_4	11	13
C2-C3-C4-C1	5.51(9)	-5.79	12.77(11)	-5.7(2)	5.3(2)	4.5(2)	-5.3(2)	22.06(7)	-4.83(8)
C3-C2-C1-C4	5.41(9)	-5.73	12.74(11)	-5.6(2)	5.3(2)	4.4(2)	-5.2(2)	22.15(7)	-4.82(8)
C2-C1-C4-C3	-5.38(9)	5.79	-12.86(11)	5.7(2)	-5.3(2)	-4.4(2)	5.3(2)	-22.23(7)	4.86(8)
C4-C3-C2-C1	-5.42(9)	5.78	-12.82(11)	5.7(2)	-5.3(2)	-4.5(2)	5.3(2)	-22.49(7)	4.91(8)
CCDC number	2192929	2192930	2192931	2192933	2192933	2192933	2192933	2192932	2089434 ⁶

5. ¹³C-NMR structure analysis

We tried to correlate the redox process to the ¹³C NMR shifts of the respective cyclobutane nuclei (Table S7). The reason behind this was that a small oxidation potential could correlate to an increased electron density at certain carbon nuclei, which would in return correlate to a high-field shift in the ¹³C NMR spectra. Although there is some evidence for this hypothesis from comparison of cyclobutane **3a** and **3c** (C1 and C4), cyclobutanes **9a-c** show almost no deviation of the ¹³C NMR shifts. Hence, ¹³C NMR analysis does not appear to be a suitable tool to describe the observations properly.

Table S7 ¹³C NMR data of the cyclobutanes ^a

compound	C1	C2	C3	C4
3a	44.1	49.4	41.8	78.9
3c	50.8	48.3	37.6	87.0
9a	51.4	52.3	40.6	84.3
9b	51.3	52.3	40.6	84.2
9c	50.8	52.4	40.5	84.1
11	52.4	53.1	41.2	42.3
13	81.8	48.7	42.6	87.0

^a Chemical shifts in ppm, C atoms as depicted in Fig. 5.

6. References

1. J. Lefarth and A. G. Griesbeck, *J. Org. Chem.*, 2022, **87**, 8028-8033.
2. M. Krejčík, M. Daněk and F. Hartl, *J. Electroanal. Chem. Interf. Electrochem.*, 1991, **317**, 179-187.
3. W. Kaim and J. Fiedler, *Chem. Soc. Rev.*, 2009, **38**, 3373-3382.
4. W. Kaim and A. Klein, *Spectroelectrochemistry*, RSC Publishing, Cambridge, 2008.
5. G. M. Sheldrick, *Acta Crystallogr A Found Adv*, 2015, **71**, 3-8.
6. J. Lefarth, J. Neudörfl and A. G. Griesbeck, *Molbank*, 2021, **2021**, M1256. <https://doi.org/10.3390/M1256>.